Journal of the mechanical behavior of biomedical materials 69 (2017) 420–434

Contents lists available at ScienceDirect

Journal of the Mechanical Behavior of Biomedical Materials

journal homepage: www.elsevier.com/locate/jmbbm

Biomechanics of the human intervertebral disc: A review of testing techniques and results

N. Newell[a,*], JP Little[b], A. Christou[a], MA Adams[c], CJ Adam[b], SD Masouros[a]

[a] Department of Bioengineering, Imperial College London, London SW7 2AZ, United Kingdom
[b] Paediatric Spine Research Group, IHBI at Centre for Children's Health Research, Queensland University of Technology, Brisbane, Australia
[c] Centre for Applied Anatomy, University of Bristol, Southwell Street, Bristol BS2 8EJ, United Kingdom

ARTICLE INFO

Keywords:
Intervertebral disc
Mechanical testing
Anulus fibrosus
Nucleus pulposus
Endplate
Material properties

ABSTRACT

Many experimental testing techniques have been adopted in order to provide an understanding of the biomechanics of the human intervertebral disc (IVD). The aim of this review article is to amalgamate results from these studies to provide readers with an overview of the studies conducted and their contribution to our current understanding of the biomechanics and function of the IVD. The overview is presented in a way that should prove useful to experimentalists and computational modellers. Mechanical properties of whole IVDs can be assessed conveniently by testing 'motion segments' comprising two vertebrae and the intervening IVD and ligaments. Neural arches should be removed if load-sharing between them and the disc is of no interest, and specimens containing more than two vertebrae are required to study 'adjacent level' effects. Mechanisms of injury (including endplate fracture and disc herniation) have been studied by applying complex loading at physiologically-relevant loading rates, whereas mechanical evaluations of surgical prostheses require slower application of standardised loading protocols. Results can be strongly influenced by the testing environment, preconditioning, loading rate, specimen age and degeneration, and spinal level. Component tissues of the disc (anulus fibrosus, nucleus pulposus, and cartilage endplates) have been studied to determine their material properties, but only the anulus has been thoroughly evaluated. Animal discs can be used as a model of human discs where uniform non-degenerate specimens are required, although differences in scale, age, and anatomy can lead to problems in interpretation.

1. Introduction

Intervertebral discs (IVDs) are pads of fibrocartilage which lie between the vertebrae of the spine. They allow the vertebral column to bend and twist (Bogduk, 2005; Humzah and Soames, 1988), and distribute compressive loading on the adjacent vertebral bodies (Adams and Roughley, 2006). The mechanical properties of discs are important because human lumbar IVDs are often physically disrupted (Vernon-Roberts et al., 1997), which may give rise to degenerative changes (Adams and Dolan, 2012; Adams and Roughley, 2006; Ferguson and Steffen, 2003) and to chronic back pain (Cheung et al., 2009; de Schepper et al., 2010). Accurate mechanical characterisation of the IVD is required to analyse injury mechanisms, and to understand how ageing and degeneration can degrade the material properties of a disc's component tissues (Ferguson and Steffen, 2003; Shan et al., 2015; Vernon-Roberts and Pirie, 1977), increasing vulnerability to injury. Other major motivations to study disc mechanics are to develop and test surgical implants such as prosthetic intervertebral discs (Cunningham et al., 2003; Lee and Goel, 2004; Lemaire et al., 1997), and to obtain accurate material properties for input into finite element models of the spine (Schmidt et al., 2013). A focus has also been on high strain-rate injuries, for example vehicle accidents, airplane ejections, and blast-related events (Panzer et al., 2011; Yoganandan et al., 1989).

The purpose of this article is to present our current understanding of the mechanical behaviour of the IVD, evaluate the methods used to test the IVD and its component tissues, and summarise the results of such tests in a manner that is useful to other experimentalists and computational modellers. The focus of the review is adult human lumbar discs. The very large number of studies concerning the human IVD poses a challenge of scale when conducting a review of this nature, and so for reasons of brevity we chose not to compare human and animal discs. However, we believe that studying animal tissues, which are often uniform and non-degenerated, can help in understanding how aspects of testing techniques (such as speed of loading, or complex loading) influence the results of experiments on human tissue, and for

* Corresponding author.
E-mail address: n.newell09@imperial.ac.uk (N. Newell).

http://dx.doi.org/10.1016/j.jmbbm.2017.01.037
Received 24 August 2016; Received in revised form 6 January 2017; Accepted 23 January 2017
Available online 31 January 2017

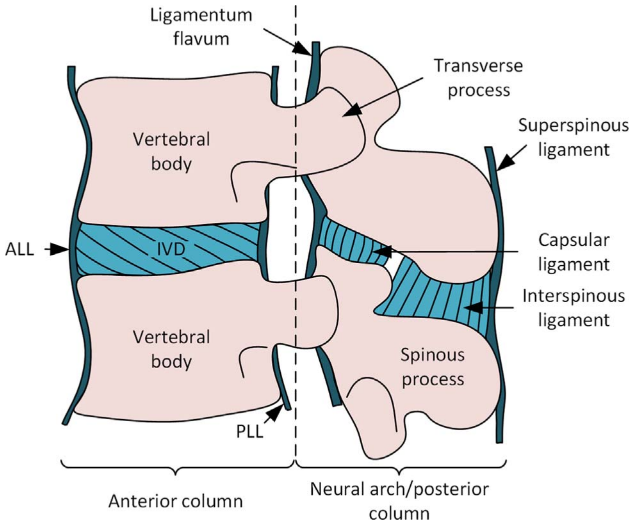

Fig. 1. Graphical representation of a motion segment; sagittal view. ALL and PLL refer to the anterior and posterior longitudinal ligaments, respectively. The capsular ligament encloses the zygapophysial joint. The intertransverse ligaments (ITLs) are not shown but they extend between upper and lower borders of the transverse processes.

this reason some data from animal studies are included here. Cadaveric discs remain the closest available representation of living human discs, and so results from cadaveric studies can most easily be translated into the clinical setting. Only meso- or macro-scale tests are considered, rather than nano- or molecular level tests.

2. Disc composition and functional anatomy

A motion segment consists of two vertebrae and an IVD (Fig. 1). The IVD has three main components (Fig. 2): a soft, deformable, nucleus pulposus (NP), which is surrounded by the fibrous concentric layers of the anulus fibrosus (AF), and bonded above and below to adjacent vertebral bodies (VBs) by the thin layers of the cartilaginous end plates (CEPs). Lumbar IVDs are the largest avascular organs in the human body. Each of the three component tissues will be considered in turn.

2.1. Nucleus pulposus (NP)

The NP is a gelatinous structure that accounts for 40–50% of the volume of the adult disc (Bayliss and Johnstone, 1992; Iatridis et al., 1996; Pooni et al., 1986) and 25–50% of the transverse cross-sectional area (Farfan et al., 1970; Nachemson, 1960; Perey, 1957). The NP has such a high water content that it exhibits a hydrostatic pressure which increases in response to compressive loading (Keyes and Compere, 1932; McNally and Adams, 1992), and this pressure generates tension in the surrounding AF (Nachemson, 1963). Its main constituents are proteoglycan, collagen and water (Antoniou et al., 1996). Proteoglycan accounts for 35–65% of the dry weight of the NP, and is important for binding water into the tissue (Dickson et al., 1967; Iatridis et al., 1996; McDevitt, 1988). Fine collagen type II fibrils, which account for 5–20% of dry weight, provide a loose, 3-dimensional fibre network, which holds the nucleus together (Eyre, 1988; Inoue and Takeda, 1975). The remainder of the dry weight of the NP is non-collagenous proteins and elastin (Eyre, 1988). NP water content decreases with age, from approximately 90–70% from the ages of 1– 80 years old (Antoniou et al., 1996; Gower and Pedrini, 1969; Kraemer et al., 1985), reflecting a similar decrease in proteoglycans.

In a healthy lumbar disc, *in vivo* pressures in the nucleus are between 460 and 1330 kPa in the seated position, 500 and 870 kPa in the standing position, and 91 and 539 kPa when lying either prone or supine (Nachemson and Morris, 1964, 1963; Sato et al., 1999; Wilke et al., 1999). The highest pressure in the nucleus (2300 kPa) was recorded in a standing subject who was flexing forwards holding a 20 kg mass (Wilke et al., 1999).

2.2. Anulus fibrosus (AF)

The AF is made up of 15–25 concentric layers – the lamellae - which are approximately 0.05–0.5 mm thick, of increasing thickness from outer to inner (Cassidy et al., 1989; Inoue and Takeda, 1975; Marchand and Ahmed, 1990). Approximately 48% of the lamellar layers are circumferentially incomplete and the percentage of incomplete layers increases with age (Marchand and Ahmed, 1990). Each layer consists of coarse and strong collagen type I fibre bundles, as in tendon, with their orientation alternating between ± 25–45° in relation to the transverse plane (Fig. 2c). The angle of inclination increases towards the centre of the disc (Cassidy et al., 1989; Horton, 1958; Hsu and Setton, 1999; Marchand and Ahmed, 1990; Pooni et al., 1986). A trans-lamellar, collagen-based bridging network provides shear resistance between adjacent lamellae (Adam et al., 2015; Melrose et al., 2008; Pezowicz et al., 2006; Schollum et al., 2008; Yu et al., 2007, 2005). The complex arrangement of collagen fibres in the AF enables it to develop tensile, 'hoop' – or circumferential – stress due to the pressure in the nucleus.

In the healthy IVD, the AF contains 65–70% water. Dry weight is approximately 20% proteoglycan, 50–70% collagen, and 2% elastin

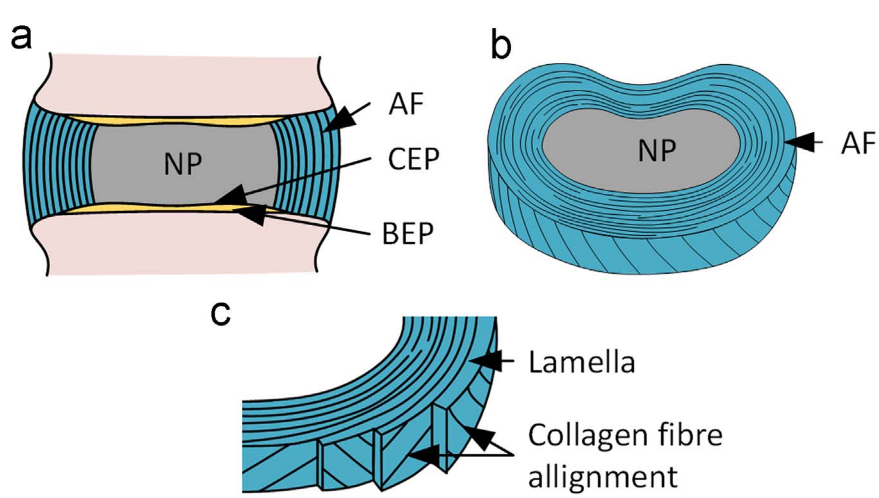

Fig. 2. Gross anatomy of a disc. (a) Cross section of a disc in the coronal plane, (b) diagram of a transversely sliced IVD and (c) diagram showing the alternating fibre alignment in successive lamellae. AF: anulus fibrosus; CEP: cartilaginous endplate; BEP: bony endplate; NP: nucleus pulposus.

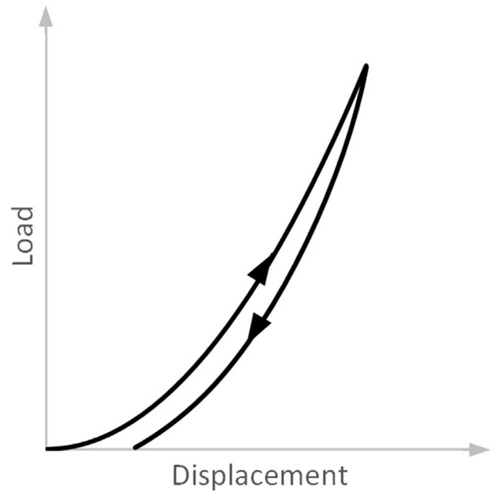

Fig. 3. Typical non-linear behaviour of a VB-disc-VB specimen subjected to uniaxial compression. The difference between the loading and unloading paths indicates viscoelastic properties (Asano et al., 1992; Koeller et al., 1986).

(Adams et al., 1977; Antoniou et al., 1996; Buckwalter, 1995; Mikawa et al., 1986; Yu et al., 2005). Moving from outer to inner AF, proteoglycan, water, and collagen type II content increases, whereas collagen type I content decreases. Mechanically, type I collagen provides strength in tension, as in tendon. Type II collagen forms a fine meshwork that binds with proteoglycans - and hence water - thus enabling the tissue to withstand large compressive forces, as in hyaline cartilage (Adams et al., 1977; Eyre and Muir, 1976; Melrose et al., 2008; Schollmeier et al., 2000). Elastin in the AF is concentrated between adjacent lamellae and helps elastic recoil following large deformations (Melrose and Ghosh, 1988; Yu et al., 2007, 2005).

2.3. Cartilaginous endplate (CEP)

The CEPs are thin layers of hyaline cartilage that bind the disc inferiorly and superiorly to the adjacent bony endplates (BEPs). They are approximately 0.6 mm thick, although they are generally thinner towards the centre where they are in contact with the NP (Roberts et al., 1997, 1989; Vernon-Roberts and Pirie, 1977). Thickness decreases with age. Dimensions in the transverse plane reflect those of the adjacent vertebral bodies, and so increase from an anterior-posterior length of 16–19 mm and lateral width of 17–29 mm in the cervical spine (Francis, 1955; Panjabi et al., 1991), rising to an anterior-posterior length of 30–36 mm and lateral width of 43–54 mm in the lumbar spine (Berry et al., 1987; Panjabi et al., 1992; Scoles et al., 1988). The CEP comprises approximately 60% water, and major dry weight constituents are collagen type II and proteoglycans. Collagen content is higher, and proteoglycan content lower, near the disc periphery (Roberts et al., 1989). The three-dimensional type II collagen network of the CEP prohibits swelling, and the relatively stable tissue is able to reduce the rate of water expulsion from the pressurised NP, while allowing nutrients to diffuse into the disc from the vertebral body (Roberts et al., 1989). The CEP is bonded weakly to a thin underlying layer of perforated cortical bone, the BEP. Under compressive loading, the pressure of the NP pressing against the CEP and BEP can cause them to bulge into the VB by up to 1 mm (Brinckmann et al., 1983; Holmes et al., 1993). This bulging increases the volume available to the NP, thereby reducing pressure in the nucleus and shifting some compressive load-bearing from the NP to the AF (Adams, 2015).

2.4. Integration between components of the IVD

Fibres of the outer AF are deeply anchored into the BEP, while fibres of the inner AF merge gradually into the CEP (Hashizume, 1980; Inoue, 1981; Rodrigues et al., 2012). The outer margin of the AF also merges into the anterior and posterior longitudinal ligaments, which are considered by some to be peripheral parts of the AF (Bogduk, 2005; Coventry et al., 1945). The NP and inner AF are connected by branches of fibres that blend the boundary between the NP and AF providing mechanical integration (Wade et al., 2012a). Fine collagen type II fibrils of the NP also insert deep into the CEP (Wade et al., 2012b).

3. Factors that can influence the spine's mechanical properties

3.1. Specimen harvesting and storage

Ideally, specimens will be harvested fresh immediately prior to testing. It is, however, common practise for specimens to be deep frozen for various amounts of time before testing. Generally, a single freeze-thaw cycle has little effect on the pressure in the NP, the stiffness or creep behaviour of the IVD (Dhillon et al., 2001; Nachemson, 1960; Panjabi et al., 1985; Smeathers and Joanes, 1988), and on the tensile behaviour of small samples of AF (Galante, 1967). After several freeze-thaw cycles, however, significant differences in joint flexibility can appear (Tan and Uppuganti, 2012). A number of animal studies have found significant mechanical differences between fresh and fresh-frozen IVDs (Bass et al., 1997; Callaghan and McGill, 1995; Sunni et al., 2014), but this may be attributable to the very high water content of young animal IVDs (Bass et al., 1997). To the authors' knowledge, the effects of precise freezing temperature and duration on the behaviour of the IVD have not been investigated.

3.2. Testing environment

Temperature and hydration should be controlled to replicate the physiological environment. At 37 °C, compressive creep is approximately 10% more than at room temperature (Koeller et al., 1986), and immersion in fluid reduces an IVD's stiffness in torsion, axial compression, and lateral bending by ~20–30% (Costi et al., 2002), possibly because of changes in inter-lamellar friction and/or hydraulic permeability. Specimen hydration during testing can be maintained by: 1) spraying water at regular intervals, 2) wrapping in saline soaked gauze, 3) testing in a humidity chamber, or 4) immersing in a saline bath. The last technique can cause problems, because cadaveric IVDs will swell by 20% if stored unloaded in a wet environment (McMillan et al., 1996), despite tension in the ligamentum flavum, which generates a pressure in the NP of approximately 70 kPa (Heuer et al., 2007; Nachemson and Evans, 1968). *In vivo*, there is a corresponding diurnal variation in hydration (and height) of the IVD of approximately 20% (Botsford et al., 1994). To allow for this, cadaveric specimens are often creep-loaded prior to testing to return the hydration of the IVD to within the physiological range (Adams, 1995; Pflaster et al., 1997; Race et al., 2000). Phosphate-buffered saline (PBS) with an osmolarity of 0.15 M achieves a stable tissue hydration *ex vivo* (Ebara et al., 1996), with IVD compressive stiffness increasing at higher osmolarity (Bezci et al., 2015).

3.3. Strain rate, preload, and preconditioning

Strain rate affects the mechanical behaviour of the viscoelastic IVD (Holzapfel et al., 2005). Generally, the quicker an IVD is compressed or rotated, the stiffer it becomes (Costi et al., 2008; Kemper et al., 2007; Smeathers and Joanes, 1988; Yingling et al., 1997). The non-linear properties of a disc mean that stiffness also increases if a compressive preload is applied prior to another mode of loading (Janevic et al., 1991), so it is usual to apply a compressive preload to simulate superincumbent body weight during testing. In multisegmental specimens – which are prone to buckling – a preload of up to 1.2 kN (depending on the segments that are being tested) is often applied as a

Table 1
Overview of human axial IVD compression tests. Where numerical values were lacking, estimates have been taken from figures. Where healthy and degenerate discs have been tested, data from the healthy discs are recorded. Where there was more than one level of preload, data refer to the largest. Incremental loading refers to forces applied in discrete steps. *Only specimens tested in axial compression are included. **Maximum loads and displacements are taken from the static compression tests, not the fatigue tests. ***A compressive preload was only applied for the dynamic tests in this study. Maximum load and displacement are taken from static tests. Minimum age was between 0 and 10 years but 10 years was reported here +Preconditioned to a displacement of 0.5 mm rather than a load, therefore data not presented. ++Compressive preload of 0.4 MPa.

Study	Type of test					Specimen		Spinal level			Rate		Test environment					Preconditioning/preloading			Results				
	Incremental loading	Single compression cycle	Cyclic/vibration	Creep	Stress relaxation	VB-disc-VB only	Motion segment	Cervical	Thoracic	Lumbar	Quasistatic	Dynamic	Saline bath	Humidity chamber	37 °C	Air	Saline soaked gauze	Compressive preload (kN)	# Preconditioning cycles	Preconditioning load (kN)	Number of specimens*	Age range	Max. load (kN)	Tested to failure?	Max. axial disp. (mm)
Virgin (1951)	☑					☑				☑	☑		☑					–	–	–	51	–	4.4	☑	1.9
Ingelmark and Ekholm (1952)	☑			☑		☑				☑	☑					☑		–	–	–	39	21–90	0.6		0.7
Hirsch and Nachemson (1954)***		☑		☑		☑	☑			☑	☑	☑				☑		1.3	–	–	94	10–90	1.0		1.8
Hirsch (1955)		☑		☑		☑				☑	☑	☑				☑		1.3	–	–	15	18–46	–		0.75
Perey (1957)		☑					☑			☑	☑	☑				☑		0.25	–	–	76	29–70	13.5	☑	–
Brown et al. (1957)	☑					☑				☑	☑					☑		–	–	–	5	–	5.8	☑	2.5
Bartelink (1957)	☑					☑				☑	☑					☑		–	–	–	10	60–80	6.2	☑	–
Nachemson (1960)	☑					☑	☑			☑	☑					☑		–	–	–	121	6–82	13.8	☑	–
Rolander (1966)	☑						☑			☑	☑					☑		–	–	–	71	4–76	6.4		–
Markolf (1972)		☑				☑	☑		☑	☑	☑			☑				–	–	–	30	21–55	2.0		13
Plaue et al. (1974)		☑				☑			☑	☑	☑					☑		–	–	–	160	21–61	8.8	☑	–
Markolf and Morris (1974)		☑		☑	☑	☑				☑	☑					☑		–	–	–	24	18–58	4.4		1.6
Kazarian (1975)	☑			☑			☑		☑	☑	☑			☑				–	–	–	32	20–65	0.5		1.5
Lin et al. (1978)	☑	☑				☑	☑			☑	☑			☑				–	–	–	19	44–81	5.8	☑	–
Berkson et al. (1979)	☑					☑	☑			☑	☑			☑				0.4	–	–	42	–	0.4		0.5
Adams and Hutton (1980)		☑					☑			☑	☑						☑	–	–	–	40	25–80	1.3		1.7
Hutton and Adams (1982)		☑					☑			☑		☑					☑	1	–	–	16	22–73	13.0	☑	–
Tencer et al. (1982)	☑					☑	☑			☑	☑			☑				0.8	–	–	14	16–57	0.8		1.3
Koeller et al.		☑	☑	☑		☑			☑	☑	☑	☑				☑		0.01	–	–	123	16–41	1.5		0.4

(continued on next page)

Table 1 *(continued)*

Study	Type of test					Specimen		Spinal level			Rate		Test environment					Preconditioning/preloading			Results				
	Incremental loading	Single compression cycle	Cyclic/vibration	Creep	Stress relaxation	VB-disc-VB only	Motion segment	Cervical	Thoracic	Lumbar	Quasistatic	Dynamic	Saline bath	Humidity chamber	37 °C	Air	Saline soaked gauze	Compressive preload (kN)	# Preconditioning cycles	Preconditioning load (kN)	Number of specimens*	Age range	Max. load (kN)	Tested to failure?	Max. axial disp. (mm)
(1984b)																									
Koeller et al. (1984a)			☑	☑		☑				☑		☑				☑		0.01	–	–	48	13–49	2.2		1.6
Burns et al. (1984)				☑			☑		☑	☑	☑			☑				–	–	–	47	27–46	0.2		–
Brinckmann and Horst (1985)		☑					☑			☑	☑					☑		–	–	–	42	18–57	8.9	☑	–
Koeller et al. (1986)			☑			☑			☑	☑		☑				☑		0.01	–	–	178	5–84	1.5		0.4
Panjabi et al. (1986)	☑						☑	☑			☑			☑				0.01	2	0.05	18	42–70	0.05		0.7
Keller et al. (1987)				☑			☑			☑	☑					☑		–	–	–	18	37–81	0.03		–
Hansson et al. (1987)			☑				☑			☑		☑				☑		–	–	–	17	37–81	4.4	☑	1.2
Smeathers and Joanes (1988)			☑				☑			☑		☑	☑		☑			0.02	1	1.0	7	27–75	1.0		0.6
Brinckmann et al. (1988)**		☑	☑				☑		☑	☑		☑		☑	☑			1.0	–	–	105	19–78	5.2	☑	1.9
Moroney et al. (1988)	☑					☑	☑	☑			☑			☑				0.05	–	–	35	–	0.1		0.1
Yoganandan et al. (1989)		☑					☑		☑	☑	☑					☑		–	–	–	9	25–86	11	☑	4
Kasra et al. (1992)			☑			☑	☑		☑	☑		☑				☑		0.68	–	0.04	7	41–85	0.7		–
Asano et al. (1992)			☑			☑	☑			☑		☑		☑				–	4	1.6	10	35–67	1.6		1.5
Holmes et al. (1993)	☑					☑				☑	☑						☑	–	–	–	17	34–74	5.5	☑	–
Izambert et al. (2003)			☑			☑				☑	☑	☑	☑		☑			0.4	300	–	8	50–72	0.4		–
Kemper et al. (2007)		☑					☑			☑		☑				☑		0.09	–	+	11	18–56	5		0.5
O'Connell et al. (2007)	☑			☑		☑				☑	☑						☑	–	–	0.02	7	22–77	1		1.9
Costi et al. (2008)			☑			☑				☑	☑	☑	☑		☑			++	–	–	9	16–60	2.1		0.25
O'Connell				☑		☑				☑	☑		☑					0.02	–	–	20	22–77	2.0		2.08

(continued on next page)

Table 1 *(continued)*

Study	Type of test					Specimen		Spinal level			Rate		Test environment				Preconditioning/preloading			Results				
	Incremental loading	Single compression cycle	Cyclic/vibration	Creep	Stress relaxation	VB-disc-VB only	Motion segment	Cervical	Thoracic	Lumbar	Quasistatic	Dynamic	Saline bath	Humidity chamber	37 °C Air	Saline soaked gauze	Compressive preload (kN)	# Preconditioning cycles	Preconditioning load (kN)	Number of specimens*	Age range	Max. load (kN)	Tested to failure?	Max. axial disp. (mm)
et al. (2011a)																								
O'Connell et al. (2011b)		☑		☑		☑				☑		☑				☑	0.02	5	0.02	14	22–80	1		–
O'Connell et al. (2011c)		☑		☑		☑				☑	☑					☑	0.02	5	0.02	19	22–76	1		0.63
Jamison et al. (2013)		☑				☑				☑		☑			☑		0.05	50	0.15	5	59–85	1		0.8
Marini et al. (2015)		☑	☑				☑			☑	☑	☑			☑		0.55	5	1.0	22	21–69	1	☑	0.9

'follower load' along a path tangent to the curve of the spine (Patwardhan et al., 2003, 2000, 1999; Stanley et al., 2004). Preconditioning, meaning cyclic loading before the intended loading protocol is applied, alleviates the effects of freezing and prolonged immobility and so ensures reproducibility. Generally, three precycles are sufficient for the response of the IVD to be consistent (Wilke et al., 1998), although some studies have incorporated thousands of preloading cycles (Costi et al., 2014; Wilke et al., 2013).

3.4. Disc age and degeneration

Age-related biochemical changes stiffen cartilage at a materials level (Bank et al., 1998), and under shear and confined compression a degenerating AF becomes stiffer (Iatridis et al., 1999, 1998; O'Connell et al., 2009). In tension, however, the accumulation of small structural defects with degeneration probably explains why AF becomes softer and weaker (Shan et al., 2015). The proteoglycan and water concentration in the NP reduces in degenerate IVDs (Buckwalter, 1995), causing the nucleus pressure to fall (Adams et al., 1996; Sato et al., 1999). The sagittal diameter of the NP reduces by approximately 50%, and the NP begins to act more like a solid than a fluid (Adams et al., 1996; Iatridis et al., 1997a; Johannessen and Elliott, 2005) so that more compressive load-bearing is transferred to the AF (Adams et al., 1996; Nachemson, 1965). With increasing age, calcification of the CEP occurs, which may contribute to disc degeneration by reducing permeability and metabolite transport (Bernick and Cailliet, 1982; Nachemson et al., 1970; Roberts et al., 1996). A degenerated disc has lost height, and intervertebral ligaments have become slack (Adams et al., 1987), so the bending stiffness of motion segments decreases with level of degeneration, and therefore age (Moroney et al., 1988; Nachemson et al., 1979; Yoganandan et al., 1989; Zhao et al., 2005). In addition, their range of motion decreases, possibly because of osteophyte growth (Al-Rawahi et al., 2011). Such profound changes in the biomechanics of the IVD render assessing the level of disc degeneration before mechanical testing an important element of the experimental protocol. Published criteria allow IVD degeneration to be graded on the basis of MRI (Johannessen et al., 2006; Pfirrmann et al., 2001; Schneiderman et al., 1987), radiographic appearance (Gordon et al., 1991), or simply from visual appearance of IVDs sectioned in the sagittal or transverse plane (Galante, 1967; Thompson et al., 1990).

3.5. Spinal level

The size and shape of IVDs vary with spinal level (Pooni et al., 1986), giving rise to systematic changes in intradiscal stresses (Dolan et al., 2013). After normalisation for size, cervical motion segments are stronger in compression but weaker in bending compared to lumbar (Przybyla et al., 2007). Lumbar IVDs have been the focus of most investigations concerned with IVD degeneration or low back pain. The mechanical responses of the five lumbar IVDs are similar in extension, lateral bending, compression, and shear (Nachemson et al., 1979), although the thicker lower lumbar discs lose more height under creep loading (Hirsch and Nachemson, 1954), and show greater anterior bulging during axial dynamic compression (Koeller et al., 1984a). Torsional stiffness of whole motion segments increases at lumbar and lower thoracic levels because of increased vertebral size, and altered orientation of the zygapophysial joints in comparison to upper thoracic and cervical levels (Markolf, 1972; Panjabi et al., 1993).

4. Biomechanical testing of functional spinal units

Tests usually involve a functional spinal unit (FSU) – or motion segment – which comprises an intact IVD still connected to its two adjacent vertebrae, with all ligaments intact. The posterior 'neural arch' region of each vertebra articulates with adjacent neural arches by means of two sliding synovial joints, the zygapophysial joints, and these

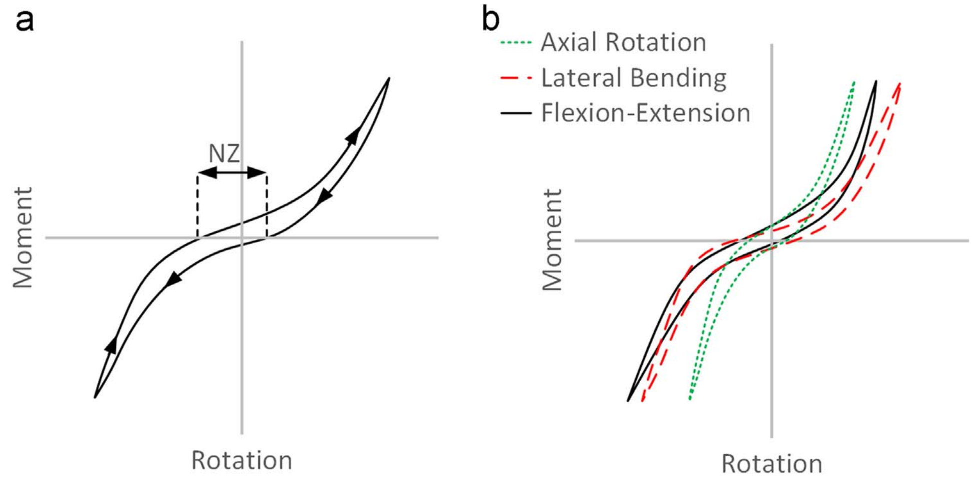

Fig. 4. (a) Typical non-linear responses of VB-disc-VB specimens subjected to bending or torsion. Note the marked hysteresis and the region of minimal stiffness (the 'neutral zone' NZ). (b) Typical curves for axial rotation, lateral bending and flexion-extension (negative rotation indicates flexion). Responses depend on spinal level, and whether the neural arches are removed.

also are preserved in a motion segment (Fig. 1). If it is required to distinguish the properties of the IVD itself from those of adjacent ligaments and zygapophysial joints, then the neural arches can be removed at the pedicles, leaving a VB-disc-VB specimen. Large specimens comprising three or more vertebrae, with all posterior structures intact, are sometimes tested because they allow adjacent-level effects to be studied, or large prostheses or fixations to be evaluated. As the focus of this review is the IVD, these experiments will not be included here. Some studies have loaded the FSU to failure in order to determine its strength for a particular mode of loading, whereas others have applied sub-failure loads in order to simulate physiological conditions. Although the two approaches have methodological differences, both are important to characterise different aspects of the biomechanical behaviour of the IVD.

Although the IVDs normally carry most of the compressive load, more than 50% can be transmitted through the neural arch of the joint complex (Pollintine et al., 2004). Load bearing by the neural arch is greater when the spine is extended than when it is flexed (Adams and Hutton, 1980; Asano et al., 1992; Hirsch and Nachemson, 1954; Lorenz et al., 1983; Shirazi-Adl and Drouin, 1987; Yang and King, 1984) and is increased when the IVDs are narrowed, either by sustained loading or by degenerative changes (Pollintine et al., 2004). To ensure that mechanical loading is applied appropriately to both anterior (vertebral bodies and IVDs) and posterior (neural arch) columns, it is important for motion segments to be secured in some stiff fixative such as dental cement before testing.

Motion segments have been tested under uniaxial compression, axial rotation, lateral bending, and flexion/extension. The following sections are categorised according to these loading modes.

4.1. Uniaxial compression

The axial compressive characteristics of the IVD have most often been investigated on lumbar VB-disc-VB specimens. A typical non-linear, viscoelastic response is shown in Fig. 3. Other experiments have considered creep (Burns et al., 1984; Hirsch, 1955; Hirsch and Nachemson, 1954; Ingelmark and Ekholm, 1952; Kazarian, 1975; Keller et al., 1987; Koeller et al., 1984a, 1984b; Markolf and Morris, 1974), stress relaxation (Markolf and Morris, 1974), vibration/dynamic compression (Asano et al., 1992; Costi et al., 2008; Hansson et al., 1987; Izambert et al., 2003; Kasra et al., 1992; Koeller et al., 1986, 1984a, 1984b; Marini et al., 2015; Smeathers and Joanes, 1988), and high loading rate properties (Hirsch, 1955; Hirsch and Nachemson, 1954; Hutton and Adams, 1982; Jamison et al., 2013; Kemper et al., 2007; Koeller et al., 1984b; Marini et al., 2015; Perey, 1957).

Table 1 summarises the methods and results from previous compression studies of the IVD. The most marked differences in methods involve the testing environment.

4.2. Bending and axial rotation

Because spinal joints are subjected to complex three-dimensional loading *in vivo*, a number of mechanical spine testers have been devised which are capable of applying combinations of compression, bending, and torsion to spinal segments *ex vivo*. Typical moment-rotation graphs (Fig. 4) show marked nonlinearity and hysteresis, and do not necessarily start at the origin because of pre-conditioning. Generally, resistance is greatest in axial rotation, followed by extension (backwards bending), lateral bending, and finally flexion (forwards bending) (Beaubien et al., 2005; Moroney et al., 1988; Schultz et al., 1979).

One key decision when applying moments to spinal joints is whether to rotate about a fixed axis, or allow the rotation axis to move and thus minimise shear. These two strategies are often described as being equivalent to 'displacement control' or 'moment control', respectively. Moments (or displacements) can be applied in a quasi-static manner by means of suspended dead-weights, or dynamically either using servo-hydraulic or electric actuators that apply moments via cables or by offsetting a compressive load. Table 2 summarises previous spinal flexion-extension, lateral bending, and axial rotation tests performed on single motion segments. Note that a number of the studies included in Table 2 have combined different modes of loading, for example Adams and Hutton (1981) combined compression and torsion, Gordon et al. (1991) combined flexion, rotation and compression, and Adams and Dolan (1996) combined compression and bending. Although not reported in Table 2, in order to reduce viscoelastic effects, specimens are often preconditioned for a number of cycles – usually 3 – until a reproducible result is achieved.

4.3. IVD injuries

Compressive overload always damages the BEP first, and vertical herniation of the NP can create Schmorl's nodes (Adams and Dolan, 2012; Brinckmann et al., 1988; Hamanishi et al., 1994). The resulting decompression of the NP may lead to internal collapse of the AF (Adams and Dolan, 2012; Gunzburg et al., 1992). For herniation to occur through the AF the IVD needs to be flexed or overloaded in

Table 2
Summary of human flexion-extension, lateral bending, and axial rotation tests on single motion segments. If a test involved more than one level of compressive preload, data refer to the largest. *Average maximum moments and rotations are not presented as the loading protocol included a combination of compression, flexion, bending or rotation. +In this study the lamina were removed but the zygapophysial joints were left intact.

Average Max. Rotation (degrees)	Flexion	6.5	–	2.1	2.5	8.4	–	5.5	–	–	5.8	–	2.9	14.8	–	11.2	1	–	10	10.4	5.3	2	7.1	5.2	–	5
	Extension	–	–	1.8	3	–	–	3	–	–	3.2	–	1.8	–	–	–	1	–	–	8.3	5.3	2	4.9	3.4	–	2
	Lateral bending	6.0	–	3	2	–	–	5.6	–	–	8.2	–	3.1	–	–	–	1.5	–	7	7.6	4.8	3	6.1	5.8	–	3
	Axial rotation	5.5	22.6	1.3	1.5	–	2.9	1.5	–	–	–	–	2.4	–	–	–	1	–	2	6.7	2.5	2	3.5	2.2	–	2
Average Max. Moment (Nm)	Flexion	2	–	6.8	8.5	49	–	10.6	–	–	–	–	8	72.8	–	59	–	–	7.5	8	–	17.6	10	7.5	–	13
	Extension	2	–	6.8	8.5	–	–	10.6	–	–	–	–	8	–	–	–	–	–	7.5	8	–	20.8	10	7.5	–	31
	Lateral bending	2	–	6.4	6	–	–	10.6	–	–	–	–	8	–	–	–	–	–	7.5	8	–	36.7	10	7.5	–	19
	Axial rotation	2	88	12.9	6	–	25	10.6	–	–	–	–	8	–	–	–	–	3	7.5	8	–	11.3	10	7.5	–	14
Static loading	Pre load (kN)	–	–	–	–	–	–	0.4	–	–	0.05	0.2	4.4	2	–	0.3	0.5	0.1	0.1	–	0.1	–	0.5	0.5	~0.6	~0.6
Tested to failure		–	☑	–	–	–	☑	–	☑	☑	☑	–	☑	☑	–	–	–	–		–	–	–	–	–	–	–
Age range		16–83	27–86	21–55	–	21–60	18–71	18–77	22–73	12–57	–	48–83	18–65	16–74	–	–	19–87	17–58	45–63	–	29–54	16–60	38–59	38–59	64–93	64–93
Number of specimens		27	66	112	11	27	25	42	61	41	35	14	13	18	–	45	8	5	7	7	9	9	8	6	14	14
Control	Displacement											☑		☑							☑	☑			☑	☑
	Moment	☑	☑	☑	☑	☑	☑	☑	☑	☑	☑	☑	☑		☑	☑	☑	☑	☑	☑			☑	☑		
Loading system	Cable Driven System														☑											
	Hanging weights and pulleys	☑	☑	☑	☑			☑			☑		☑													
	6-axis testing machine																☑		☑		☑	☑	☑	☑	☑	☑
	Offset compressive loading					☑	☑		☑	☑		☑		☑		☑		☑		☑						
	Torque motors																									
Load application	Constant rate loading					☑	☑		☑	☑		☑		☑	☑	☑	☑	☑	☑	☑	☑	☑	☑	☑	☑	☑
	Incremental loading	☑	☑	☑	☑			☑			☑		☑													
Spine segment	Cervical										☑				–											
	Thoracic	☑	☑	☑	☑										–											
	Lumbar			☑		☑	☑	☑	☑	☑		☑	☑	☑	–	☑	☑	☑	☑	☑	☑	☑	☑	☑	☑	☑
Type of specimen	VB-disc-VB only	☑	☑	☑		☑	☑	☑			☑		☑	☑	–		☑			☑	☑	☑	☑	☑	☑	
	With posterior elements	☑	☑	☑	☑	☑	☑	☑	☑	☑	☑	☑	☑	☑	–	☑	☑	☑	☑				☑	☑	☑	
Loading mode	Flexion-Extension	☑	☑	☑	☑	☑		☑	☑	☑	☑	☑	☑	☑	☑	☑	☑	☑	☑	☑	☑	☑	☑	☑	☑	☑

(continued on next page)

Table 2 (*continued*)

Study	Lateral Bending	Axial Rotation
White (1969)	☑	☑
Farfan et al. (1970)	☑	☑
Markolf (1972)**	☑	☑
Panjabi et al. (1976)	☑	☑
Schultz et al. (1979)		
Adams et al. (1980)		☑
Adams and Hutton (1981)	☑	☑
Adams and Hutton (1982)**	☑	
Adams and Hutton (1983)		
Moroney et al. (1988)	☑	☑
Janevic et al. (1991)		☑
Gordon et al. (1991)*	☑	☑
Adams et al. (1994)		
Crawford et al. (1995)	☑	☑
Tencer et al. (1995)		
Adams and Dolan (1996)	☑	☑
Gardner-Morse and Stokes (2004)	☑	☑
Beaubien et al. (2005)	☑	☑
Spenciner et al. (2006)	☑	☑
Costi et al. (2007)	☑	☑
Costi et al. (2008)	☑	☑
Heuer et al. (2007)	☑	☑
Heuer et al. (2008)	☑	☑
Amin et al. (2016a)	☑	☑
Amin et al. (2016b)	☑	☑

multiple modes simultaneously; the likelihood of herniation to occur under load is higher at high loading rates (Adams and Hutton, 1982; Wade et al., 2014, 2015). Excessive torsion damages the neural arch (Adams and Hutton, 1981), and may cause delamination of the outer anulus (Farfan et al., 1970). Complex loading in bending and compression can lead to radial fissures (Adams and Hutton, 1983), and disc prolapse ('slipped disc'), either in a single loading cycle (Adams and Hutton, 1982), or by fatigue failure (Adams and Hutton, 1985). Axial rotation probably enhances the vulnerability of the posterior portions of the IVD to damage, and reduces the load required to cause disc failure (Callaghan and McGill, 2001; Drake et al., 2005; Gordon et al., 1991; Pearcy and Hindle, 1991; Shirazi-Adl et al., 1986; Veres et al., 2010).

5. Material properties of IVD constituent tissue

To gain a full understanding of the mechanical behaviour of the IVD as a whole, it is important to understand the behaviour of its component tissues.

5.1. Nucleus pulposus (NP)

Material properties of the NP are poorly characterised, reflecting the fact that it is extremely difficult to test in isolation. There is even debate as to whether it behaves predominantly as a solid or a liquid, with solid behaviour being more apparent under dynamic conditions (Iatridis et al., 1996). In tension, the tissue is so non-linear that it has been likened to a 'tethered fluid' (Skrzypiec et al., 2007a; Wade et al., 2012a). NP properties have been measured in confined compression (Johannessen and Elliott, 2005; Yang and Kish, 1988), unconfined compression (Cloyd et al., 2007), and shear (Bodine et al., 1982; Iatridis et al., 1997b). In confined compression, reported effective modulus of human, non-degenerate NP is 1.0 MPa (Johannessen and Elliott, 2005), and bulk modulus is 1720 MPa (Yang and Kish, 1988). Although the behaviour of the NP is not linearly elastic, Cloyd et al. (2007) reported a modulus from the 'linear' region of the stress-strain response in unconfined compression of 5.4 kPa. Shear moduli have been reported between 7 and 50 kPa (Bodine et al., 1982; Iatridis et al., 1997b).

5.2. Anulus fibrosus (AF)

Table 3 summarises mechanical characterisation studies of the human AF according to test protocol, type of specimen, loading rate, direction of loading, and method of gripping. Galante (1967) also tested multiple lamina specimens at various angles, including across fibre, however these results have not been included in Table 3 in order to avoid confusion with results obtained from single layer cross-fibre and in-line-with-fibre specimens.

A number of studies in Table 3 found that the outer and anterior regions of the AF were considerably stiffer than the inner and posterior regions of the AF (Ebara et al., 1996; Elliott and Setton, 2001; Holzapfel et al., 2005; Shan et al., 2015; Skaggs et al., 1994). In tension, the AF is stiffest along the axis of the fibres (average modulus=183 MPa), followed by the circumferential direction (16 MPa), and finally the radial, axial and cross fibre directions (where average moduli were 0.3, 2.6 and 0.2 MPa, respectively). In circumferential tension the average failure stress was 2.7 MPa and the average failure strain was 0.3. The maximum strain rate at which the tensile behaviour of the AF has been investigated is 4%/s which may be considered to be relatively low compared to the strain rates expected in many physiological activities and indeed in injurious scenarios. The tensile properties of small anulus specimens also depend on specimen size, because small excised specimens sustain proportionally greater disruption to the collagen network (Adams and Green, 1993).

Gripping small excised specimens of soft tissue is a challenge,

Table 3
Overview of tensile tests on the human AF. Where specimens from different regions of the AF were included, an average is recorded. Where numerical data were not presented, values have been estimated from figures. *Circumferential failure stress/strain is reported here, the along fibre (multiple lamella) failure stress was higher at 8.8 MPa and the failure strain was lower at 0.25. +Along fibre, rather than radial failure stress and failure strain is reported here, radial failure stress was lower and failure strain was higher (0.187 MPa and 1.61).

Study		Galante (1967)	Wu and Yao (1976)	Panagiotacopulos et al. (1987)	Marchand and Ahmed (1989)	Adams and Green (1993)	Green et al. (1993)	Best et al. (1994)	Skaggs et al. (1994)	Acaroglu et al. (1995)	Ebara et al. (1996)	Fujita et al. (1997)	Iatridis et al. (1998)	Iatridis et al. (1999)	Fujita et al. (2000)	Klisch and Lotz (2000)	Elliott and Setton (2001)	Bass et al. (2004)	Wagner and Lotz (2004)	Holzapfel et al. (2005)	Guerin and Elliott (2006)	Skrzypiec et al. (2007b)	Smith et al. (2008)	O'Connell et al. (2009)	Sen et al. (2012)	Shan et al. (2015)
Results	Strain rate (%/s)	0.8	0.14	–	0.08	–	–	–	0.01	.001	0.01	0.5	0.01	–	–	0.05	0.01	0.01	0.01	0.01	0.01	0.15	0.25	0.01	4.00	0.2
	Av. failure strain	0.3*	0.25	–	0.6+	–	0.4	–	0.12	0.2	0.13	0.8	–	–	–	–	–	–	–	–	–	0.49	–	–	–	0.44
	Av. failure stress (MPa)	3.4*	3.8	–	110+	–	6	–	6.3	1.1	1.5	0.2	–	–	–	–	–	–	–	–	–	4.5	–	–	–	2.1
	Radial modulus (MPa)	–	–	–	0.16	–	–	0.4	–	–	–	0.5	0.5	–	–	0.1	0.45	–	–	–	–	–	0.22	0.32	–	–
	Circ. modulus (MPa)	–	28	–	–	–	–	–	–	12.7	21.3	–	–	–	0.03	–	11.5	15.7	13.2	–	29.2	10.3	–	21.8	3.23	8.72
	Axial modulus (MPa)	–	–	–	–	–	17.2	–	–	–	–	–	0.5	0.15	0.06	0.12	0.89	1.2	–	–	–	–	–	0.37	–	–
	Along fibre mod. (MPa)	–	–	–	410	–	–	–	90	–	–	–	–	–	–	–	–	–	–	50.2	–	–	–	–	–	–
	Cross fibre mod. (MPa)	–	–	–	–	–	–	–	–	–	–	–	–	–	–	–	–	–	–	0.22	–	–	–	–	–	–
	Age range (years)	5–78	20–30	–	39–41	19–71	19–71	30–45	–	2–88	26–53	50–70	12–83	–	35–71	28–41	27–72	28–50	16–38	30–79	–	48–91	16–87	36–80	25–80	25–64
	Num. of specimens	592	30	8	168	11	22	6	59	48	60	183	44	13	86	32	60	5	11	46	14	132	32	13	8	1969
Gripping method	Other							☑					☑	☑		☑									☑	
	Bone-Disc-Bone potted					☑	☑																			
	Rakes/hooks																	☑	☑							
	Cyanoacrylate		☑						☑			☑			☑							☑	☑			☑
	Sand/polishing paper								☑	☑	☑	☑			☑		☑			☑		☑	☑			☑
	Loaded clamps	☑	☑	☑	☑				☑	☑	☑	☑			☑		☑	☑		☑	☑	☑		☑		☑
Direction of loading	Radial				☑			☑				☑	☑			☑	☑						☑	☑		
	Circumferential	☑	☑	☑						☑	☑				☑		☑	☑	☑		☑	☑		☑	☑	☑
	Axial	☑				☑	☑						☑	☑	☑	☑	☑	☑						☑		
	Along fibre axis	☑		☑	☑				☑											☑						
	Cross fibre																			☑						
Rate of testing	Quasistatic	☑	☑	☑	☑	☑	☑	☑	☑	☑	☑	☑	☑	☑	☑	☑	☑	☑	☑	☑	☑	☑	☑	☑		☑
	Dynamic											☑		☑											☑	
Type of specimen	Single Lamella								☑						☑					☑					☑	
	Multiple Lamellae	☑	☑	☑	☑	☑	☑	☑		☑	☑	☑	☑	☑	☑	☑	☑	☑	☑		☑	☑	☑	☑		☑
Type of test	Tension	☑	☑	☑	☑	☑	☑		☑	☑	☑	☑					☑	☑	☑	☑	☑	☑	☑	☑	☑	☑
	Compression							☑					☑			☑			☑							
	Shear													☑	☑											

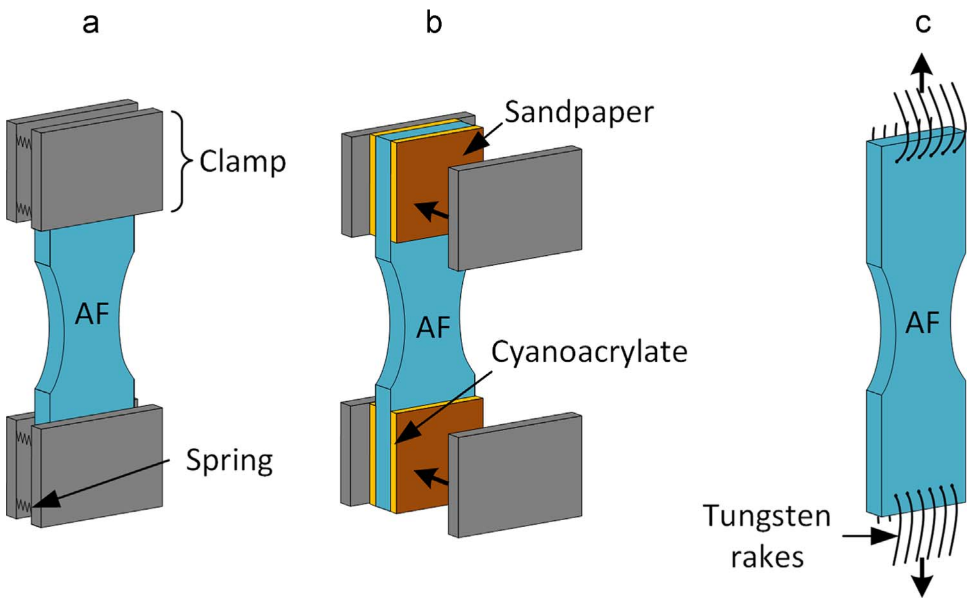

Fig. 5. Diagrammatic representations of three common gripping methods used when testing AF specimens. (a) Spring loaded clamps, (b) clamps with sandpaper and cyanoacrylate and (c) tungsten rakes pierced into the specimen.

particularly in uniaxial tension tests where slippage is common. Loaded clamps are often used, particularly in combination with sandpaper or polishing paper, and cyanoacrylate glue (Fujita et al., 2000, 1997; Shan et al., 2015; Skaggs et al., 1994; Skrzypiec et al., 2007b; Smith et al., 2008). Tungsten rakes, wire rods pierced through the specimen, and aluminium rings clamped around the specimen have also been used (Bass et al., 2004; Wagner and Lotz, 2004). Slippage can give rise to large errors if specimen strain is calculated from displacement of the clamps. Measuring strain optically eliminates this problem, and enables regional variations in strain to be studied (Masouros et al., 2009). Diagrammatic representations of common gripping methods are presented in Fig. 5.

5.3. Cartilaginous (CEP) and bony (BEP) endplates

The CEP has not been studied extensively either, possibly because the tissue layer is so thin rendering it difficult to harvest. CEP fragments often appear in IVD herniations, which may be because the CEP-vertebra junction is very weak or because the CEP-NP integration is relatively strong (Lama et al., 2014; Wade et al., 2014). CEP strength has been characterised by a number of studies in order to understand failure mechanisms and to help design interbody implants or grafts (Grant et al., 2001; Perey, 1957). Although the properties of the CEP are not linearly elastic, a modulus value has been estimated as 23.8 MPa (Yamada, 1970).

Indentation tests show that the underlying BEP is stiffest and strongest around the periphery of the VB, with stiffness of healthy BEPs in the region of 75–175 N/mm (Grant et al., 2001; Liu et al., 2016). Stiffness and strength both decrease in the presence of IVD degeneration (Liu et al., 2016). Deflection of whole lumbar endplates BEPs has also been studied during compression of VB-disc-VB specimens where, at the centre of the caudal endplate; the compliance is approximately 0.1 mm/kN (Holmes et al., 1993). Failure is more common in the weaker cranial BEP, because it is 14% thinner than the caudal BEP and supported by less dense trabecular bone (Zhao et al., 2009).

6. Discussion

This paper has provided a detailed review of the techniques used, and results obtained by, studies that have attempted to characterise mechanically the IVD. The IVD is a complex structure which changes quite markedly with age and degeneration, and IVD dysfunction can adversely affect quality of life. Disc mechanical responses are sensitive to the testing environment and boundary conditions applied, so care must be taken to ensure that applied loading is appropriate for each specific research question. A wide range of testing techniques have been used, but a consensus is emerging regarding such details as the need to precondition specimens to obtain a more repeatable response during testing, and the need to take account of posture, loading rate, and disc age and degeneration when comparing results between experiments. Future experimental studies will benefit from finding a similar consensus regarding testing environment (humidity, temperature) and methods of pre-test storage. We suggest that future work is required in the following specific research areas: 1) the influence of spinal level on the mechanical properties of constitutive components of the motion segment; 2) the responses of the IVD to complex (combined) loading modes, particularly in relation to injury mechanisms; 3) mechanical properties of the nucleus pulposus at varying strain rates and levels of degeneration; and 4) high strain-rate material properties of the anulus fibrosus.

It was apparent when performing this review that breakthroughs in our understanding of the biomechanics of the IVD often coincided with the introduction of a new measuring capability or technology. For example, new techniques for imaging the disc, for applying complex loading to cadaveric specimens, and for quantifying stress and strain distributions within discs have contributed greatly to our understanding of how discs function and fail. This effect is likely to continue into the future, and it emphasises the importance of understanding variations in past techniques in order to develop new ones.

Acknowledgements

This work was supported by the EPSRC, First Grant Scheme, EP/M022242/1. Contributions to this work were made under the auspices of The Royal British Legion Centre for Blast Injury Studies at Imperial College London; therefore the financial support of the Royal British Legion for AC and SM is gratefully acknowledged.

References

Acaroglu, E.R., Iatridis, J.C., Setton, L.A., Foster, R.J., Mow, V.C., Weidenbaum, M., 1995. Degeneration and aging affect the tensile behavior of human lumbar anulus fibrosus. Spine (Phila. Pa. 1976) 20, 2690–2701.

Adam, C., Rouch, P., Skalli, W., 2015. Inter-lamellar shear resistance confers compressive stiffness in the intervertebral disc: an image-based modelling study on the bovine caudal disc. J. Biomech. 48, 4303–4308.
Adams, M.A., 2015. Intervertebral disc tissues. In: Derby, B., Akhtar, R. (Eds.), Mechanical Properties of Aging Soft Tissues. Springer International Publishing, 7–35.
Adams, M.A., 1995. Mechanical testing of the spine. An appraisal of methodology, results and conclusions. Spine (Phila. Pa. 1976) 20, 2151–2156.
Adams, M.A., Dolan, P., 2012. Intervertebral disc degeneration: evidence for two distinct phenotypes. J. Anat. 221, 497–506.
Adams, M.A., Dolan, P., 1996. Time-dependent changes in the lumbar spine's resistance to bending. Clin. Biomech. 11, 194–200.
Adams, M.A., Dolan, P., Hutton, W.C., 1987. Diurnal variations in the stresses on the lumbar spine. Spine (Phila. Pa. 1976) 12, 130–137.
Adams, M.A., Green, T.P., 1993. Tensile properties of the annulus fibrosus. I. The contribution of fibre-matrix interactions to tensile stiffness and strength. Eur. Spine J 2, 203–208.
Adams, M.A., Green, T.P., Dolan, P., 1994. The strength in anterior bending of lumbar intervertebral discs. Spine (Phila. Pa. 1976) 19, 2197–2203.
Adams, M.A., Hutton, W.C., 1985. Gradual disc prolapse. Spine (Phila. Pa. 1976) 10, 524–531.
Adams, M.A., Hutton, W.C., 1983. The effect of fatigue on the lumbar intervertebral disc. J. Bone Jt. Surg. 65–B, 199–203.
Adams, M.A., Hutton, W.C., 1982. Prolapsed intervertebral disc: a hyperflexion injury. Spine (Phila. Pa. 1976) 7, 184–191.
Adams, M.A., Hutton, W.C., 1981. The relevance of torsion to the mechanical derangement of the lumbar spine. Spine (Phila. Pa. 1976) 6, 241–248.
Adams, M.A., Hutton, W.C., 1980. The effect of posture on the role of the apophysial joints in resisting intervertebral compressive forces. J. Bone Jt. Surg. Br. 62, 358–362.
Adams, M.A., Hutton, W.C., Stott, J.R.R., 1980. The resistance to flexion of the lumbar intervertebral joint. Spine (Phila. Pa. 1976) 5, 245–253.
Adams, M.A., McNally, D.S., Dolan, P., 1996. "Stress" distributions inside intervertebral discs. The effects of age and degeneration. J. Bone Jt. Surg. Br. 78, 965–972.
Adams, M.A., Roughley, P.J., 2006. What is intervertebral disc degeneration, and what causes it? Spine (Phila. Pa. 1976) 31, 2151–2161.
Adams, P., Eyre, D.R., Muir, H., 1977. Biochemical aspects of development and ageing of human lumbar intervertebral discs. Rheumatol. Rehabil. 16, 22–29.
Al-Rawahi, M., Luo, J., Pollintine, P., Dolan, P., Adams, M.A., 2011. Mechanical function of vertebral body osteophytes, as revealed by experiments on cadaveric spines. Spine (Phila. Pa. 1976) 36, 770–777.
Amin, D.B., Sommerfeld, D., Lawless, I.M., Stanley, R.M., Ding, B., Costi, J.J., 2016a. The effect of six degree of freedom loading sequence on the in-vitro compressive properties of human lumbar spine segments. J. Biomech. 49, 3407–3414.
Amin, D.B., Sommerfeld, D., Lawless, I.M., Stanley, R.M., Ding, B., Costi, J.J., 2016b. Effect of degeneration on the six degree of freedom mechanical properties of human lumbar spine segments. J. Orthop. Res. 34, 1399–1409.
Antoniou, J., Steffen, T., Nelson, F., Winterbottom, N., Hollander, A.P., Poole, R.A., Aebi, M., Alini, M., 1996. The human lumbar intervertebral disc: evidence for changes in the biosynthesis and denaturation of the extracellular matrix with growth, maturation, ageing, and degeneration. J. Clin. Invest. 98, 996–1003.
Asano, S., Kaneda, K., Umehara, S., Tadano, S., 1992. The mechanical properties of the human L4-5 functional spinal unit during cyclic loading: the structural effects of the posterior elements. Spine (Phila. Pa. 1976) 17, 1343–1352.
Bank, R.A., Bayliss, M.T., Lafeber, F.P.J.G., Maroudas, A., Tekoppele, J.M., 1998. Ageing and zonal variation in post-translational modification of collagen in normal human articular cartilage: the age-related increase in non-enzymatic glycation affects biomechanical properties of cartilage. Biochem. J 330, 345–351.
Bartelink, D.L., 1957. The role of abdominal pressure in relieving the pressure on the lumbar intervertebral discs. J. Bone Jt. Surg. Br. 39–B, 718–725.
Bass, E., Duncan, N., Hariharan, J., 1997. Frozen storage affects the compressive creep behavior of the porcine intervertebral disc. Spine (Phila. Pa. 1976) 22, 2867–2876.
Bass, E.C., Ashford, F.A., Segal, M.R., Lotz, J.C., 2004. Biaxial testing of human annulus fibrosus and its implications for a constitutive formulation. Ann. Biomed. Eng. 32, 1231–1242.
Bayliss, M., Johnstone, B., 1992. Biochemistry of the intervertebral disc. In: Jayson, M.I.V., Dixon, A.S.J. (Eds.), The Lumbar Spine and Back Pain. Churchill Livingstone, Edinburgh, 111–131.
Beaubien, B.P., Derincek, A., Lew, W.D., Wood, K.B., 2005. In vitro, biomechanical comparison of an anterior lumbar interbody fusion with an anteriorly placed, low-profile lumbar plate and posteriorly placed pedicle screws or translaminar screws. Spine (Phila. Pa. 1976) 30, 1846–1851.
Berkson, M.H., Nachemson, A., Schultz, A.B., 1979. Mechanical properties of human lumbar spine motion segments -Part II: responses in compression and shear; influence of gross morphology. J. Biomech. Eng. 101, 53–57.
Bernick, S., Cailliet, R., 1982. Vertebral end-plate changes with aging of human vertebrae. Spine (Phila. Pa. 1976) 7, 97–102.
Berry, J., Moran, J., Berg, W., Steffee, A., 1987. A morphometric study of human lumbar and selected thoracic vertebrae. Spine (Phila. Pa. 1976) 12, 362–367.
Best, B.A., Guilak, F., Setton, L.A., Zhu, W., Saed-Nejad, F., Ratcliffe, A., Weidenbaum, M., Mow, V.C., 1994. Compressive mechanical properties of the human annulus fibrosus and their relationship to biochemical composition. Spine (Phila. Pa. 1976) 19, 212–221.
Bezci, S.E., Nandy, A., O'Connell, G.D., 2015. Effect of hydration on healthy intervertebral disk mechanical stiffness. J. Biomech. Eng. 137, 101007-1–101007–8.
Bodine, A.J., Ashany, D., Hayes, W.C., White, A.A., 1982. Viscoelastic shear modulus of the human intervertebral disc. Trans. Orthop. Res. Soc. 7, 237.
Bogduk, N., 2005. Clinical Anatomy of the Lumbar Spine and Sacrum Fourth ed.. Elsevier Health Sciences, London, UK.
Botsford, D., Esses, S., Ogilvie-Harris, D., 1994. In vivo diurnal variation in intervertebral disc volume and morphology. Spine (Phila. Pa. 1976) 19, 935–940.
Brinckmann, P., Biggemann, M., Hilweg, D., 1988. Fatigue fracture of human lumbar vertebrae. Clin. Biomech. 3, S1–S23.
Brinckmann, P., Frobin, W., Hierholzer, E., Horst, M., 1983. Deformation of the vertebral end-plate under axial loading of the spine. Spine (Phila. Pa. 1976) 8, 851–856.
Brinckmann, P., Horst, M., 1985. The influence of vertebral body fracture, intradiscal injection, and partial discectomy on the radial bulge and height of human lumbar discs. Spine (Phila. Pa. 1976) 10, 138–145.
Brown, T., Hansen, R.J., Yorra, A.J., 1957. Some mechanical tests on the lumbosacral spine with particular reference to the intervertebral discs; a preliminary report. J. Bone Jt. Surg. Am. 39, 1135–1164.
Buckwalter, J.A., 1995. Aging and degeneration of the human intervertebral disc. Spine (Phila. Pa. 1976) 20, 1307–1314.
Burns, M.L., Kaleps, I., Kazarian, L.E., 1984. Analysis of compressive creep behavior of the vertebral unit subjected to a uniform axial loading using exact parametric solution equations of Kelvin-solid models - Part II. Rhesus monkey intervertebral joints. J. Biomech. 17, 131–136.
Callaghan, J.P., McGill, S.M., 2001. Intervertebral disc herniation: studies on a porcine model exposed to highly repetitive flexion/extension motion with compressive force. Clin. Biomech. 16, 28–37.
Callaghan, J.P., McGill, S.M., 1995. Frozen storage increases the ultimate compressive load of porcine vertebrae. J. Orthop. Res. 13, 809–812.
Cassidy, J.J., Hiltner, a, Baer, E., 1989. Hierarchical structure of the intervertebral disc. Connect. Tissue Res. 23, 75–88.
Cheung, K.M.C., Karppinen, J., Chan, D., Ho, D.W.H., Song, Y., Sham, P., Cheah, K.S.E., Leong, J.C.Y., Luk, K.D.K., 2009. Prevalence and pattern of lumbar magnetic resonance imaging changes in a population study of one thousand forty-three individuals. Spine (Phila. Pa. 1976) 34, 934–940.
Cloyd, J.M., Malhotra, N.R., Weng, L., Chen, W., Mauck, R.L., Elliott, D.M., 2007. Material properties in unconfined compression of human nucleus pulposus, injectable hyaluronic acid-based hydrogels and tissue engineering scaffolds. Eur. Spine J 16, 1892–1898.
Costi, J., Heinze, K., Lawless, I., Stanley, R., Freeman, B., 2014. Do combined compression, flexion and axial rotation place degenerated discs at risk of posterolateral herniation? Measurement of 3D lumbar intervertebral disc internal strains during repetitive loading. Bone Jt. J. Orthop. Proc. Suppl. 96–B, 219.
Costi, J.J., Hearn, T.C., Fazzalari, N.L., 2002. The effect of hydration on the stiffness of intervertebral discs in an ovine model. Clin. Biomech. 17, 446–455.
Costi, J.J., Stokes, I.A., Gardner-Morse, M., Laible, J.P., Scoffone, H.M., Iatridis, J.C., 2007. Direct measurement of intervertebral disc maximum shear strain in six degrees of freedom: motions that place disc tissue at risk of injury. J. Biomech. 40, 2457–2466.
Costi, J.J., Stokes, I.A., Gardner-Morse, M.G., Iatridis, J.C., 2008. Frequency-dependent behaviour of the intervertebral disc in response to each of six degree of freedom dynamic loading: solid phase and fluid phase contributions. Spine (Phila. Pa. 1976) 33, 1731–1738.
Coventry, M., Ghormley, R., Kernohan, J., 1945. The intervertebral disc: its anatomy and pathology. Part I. anatomy, development and physiology. J. Bone Jt. Surg. 27, 105–112.
Crawford, N.R., Brantley, A.G.U., Dickman, C.A., Koeneman, E.J., 1995. An apparatus for applying pure nonconstraining moments to spine segments in vitro. Spine (Phila. Pa. 1976) 20, 2097–2100.
Cunningham, B.W., Gordon, J.D., Dmitriev, A.E., Hu, N., McAfee, P.C., 2003. Biomechanical evaluation of total disc replacement arthroplasty: an in vitro human cadaveric model. Spine (Phila. Pa. 1976) 28, S110–S117.
de Schepper, E.I.T., Damen, J., van Meurs, J.B.J., Ginai, A.Z., Popham, M., Hofman, A., Koes, B.W., Bierma-Zeinstra, S.M., 2010. The association between lumbar disc degeneration and low back pain: the influence of age, gender, and individual radiographic features. Spine (Phila. Pa. 1976) 35, 531–536.
Dhillon, N., Bass, E.C., Lotz, J.C., 2001. Effect of frozen storage on the creep behavior of human intervertebral discs. Spine (Phila. Pa. 1976) 26, 883–888.
Dickson, I.R., Happey, F., Pearson, C.H., Naylor, A., Turner, R.L., 1967. Variations in the protein components of human intervertebral disk with age. Nature 215, 52–53.
Dolan, P., Luo, J., Pollintine, P., Landham, P.R., Stefanakis, M., Adams, M.A., 2013. Intervertebral disc decompression following endplate damage: implications for disc degeneration depend on spinal level and age. Spine (Phila. Pa. 1976) 38, 1473–1481.
Drake, J.D.M., Aultman, C.D., McGill, S.M., Callaghan, J.P., 2005. The influence of static axial torque in combined loading on intervertebral joint failure mechanics using a porcine model. Clin. Biomech. 20, 1038–1045.
Ebara, S., Iatridis, J.C., Setton, L.A., Foster, R.J., Mow, V.C., Weidenbaum, M., 1996. Tensile properties of nondegenerate human lumbar anulus fibrosus. Spine (Phila. Pa 1976) 21, 452–461.
Elliott, D.M., Setton, L.A., 2001. Anisotropic and inhomogeneous tensile behavior of the human anulus fibrosus: experimental measurement and material model predictions. J. Biomech. Eng. 123, 256–263.
Eyre, D.R., 1988. Collagens of the disc. In: Ghosh, P. (Ed.), The Biology of the Intervertebral Disc. CRC Press, Boca Raton, Florida, USA, 171–189.
Eyre, D.R., Muir, H., 1976. Types I and II collagens in intervertebral disc. Interchanging radial distributions in annulus fibrosus. Biochem. J 157, 267–270.
Farfan, H.F., Cossette, J.W., Robertson, G.H., 1970. The effects of torsion on the lumbar intervertebral joints: the role of torsion in the production of disc degeneration. J.

Bone Jt. Surg. 52, 468–497.
Ferguson, S.J., Steffen, T., 2003. Biomechanics of the aging spine. Eur. Spine J. 12, S97–S103.
Francis, C., 1955. Dimensions of the cervical vertebrae. Anat. Rec. 122, 603–609.
Fujita, Y., Duncan, N.A., Lotz, J.C., 1997. Radial tensile properties of the lumbar annulus fibrosus are site and degeneration dependent. J. Orthop. Res. 15, 814–819.
Fujita, Y., Wagner, D.R., Biviji, A.A., Duncan, N.A., Lotz, J.C., 2000. Anisotropic shear behavior of the annulus fibrosus: effect of harvest site and tissue prestrain. Med. Eng. Phys. 22, 349–357.
Galante, J.O., 1967. Tensile properties of the human lumbar annulus fibrosus. Acta Orthop. Scand. Suppl. (Suppl. 100), S1–S91.
Gardner-Morse, M.G., Stokes, I.A.F., 2004. Structural behavior of human lumbar spinal motion segments. J. Biomech. 37, 205–212.
Gordon, S.J., Yang, K.H., Mayer, P.J., Mace, A.H., Kish, V.L., Radin, E.L., 1991. Mechanism of disc rupture. A preliminary report. Spine (Phila. Pa. 1976) 16, 450–456.
Gower, W., Pedrini, V., 1969. Age-related variations in protein polysaccharides from human nucleus pulposus, annulus fibrosus, and costal cartilage. J Bone Jt. Surg. Am. 51, 1154–1162.
Grant, J.P., Oxland, T.R., Dvorak, M.F., 2001. Mapping the structural properties of the lumbosacral vertebral endplates. Spine (Phila. Pa. 1976) 26, 889–896.
Green, T.P., Adams, M.A., Dolan, P., 1993. Tensile properties of the annulus fibrosus. Eur. Spine J. 2, 209–214.
Guerin, H.A.L., Elliott, D.M., 2006. Degeneration affects the fiber reorientation of human annulus fibrosus under tensile load. J. Biomech. 39, 1410–1418.
Gunzburg, R., Parkinson, R., Moore, R., 1992. A cadaveric study comparing discography, magnetic resonance imaging, histology, and mechanical behavior of the human lumbar disc. Spine (Phila. Pa. 1976) 17, 417–426.
Hamanishi, C., Kawabata, T., Yosii, T., Tanaka, S., 1994. Schmorl's nodes on magnetic resonance imaging. Their incidence and clinical relevance. Spine (Phila. Pa. 1976) 19, 450–453.
Hansson, T., Keller, T.S., Spengler, D.M., 1987. Mechanical behavior of the human lumbar spine. II. Fatigue strength during dynamic compressive loading. J. Orthop. Res. 5, 479–487.
Hashizume, H., 1980. Three-dimensional architecture and development of lumber intervertebral discs. Acta Med. 34, 301–314.
Heuer, F., Schmidt, H., Klezl, Z., Claes, L., Wilke, H.J., 2007. Stepwise reduction of functional spinal structures increase range of motion and change lordosis angle. J. Biomech. 40, 271–280.
Heuer, F., Schmidt, H., Wilke, H.J., 2008. Stepwise reduction of functional spinal structures increase disc bulge and surface strains. J. Biomech. 41, 1953–1960.
Hirsch, C., 1955. The reaction of intervertebral discs to compression forces. J. Bone Jt. Surg. 37, 1188–1196.
Hirsch, C., Nachemson, A., 1954. New observations on the mechanical behavior of lumbar discs. Acta Orthop. Scand. 23, 254–283.
Holmes, A.D., Hukins, D.W., Freemont, A.J., 1993. End-plate displacement during compression of lumbar vertebra-disc-vertebra segments and the mechanism of failure. Spine (Phila. Pa. 1976) 18, 128–135.
Holzapfel, G.A., Schulze-Bauer, C.A.J., Feigl, G., Regitnig, P., 2005. Single lamellar mechanics of the human lumbar anulus fibrosus. Biomech. Model. Mechanobiol. 3, 125–140.
Horton, W.G., 1958. Further observations on the elastic mechanism of the intervertebral disc. J. Bone Jt. Surg. Br] 40, 552–557.
Hsu, E.W., Setton, L. a, 1999. Diffusion tensor microscopy of the intervertebral disc anulus fibrosus. Magn. Reson. Med. 41, 992–999.
Humzah, M.D., Soames, R.W., 1988. Human intervertebral disc: structure and function. Anat. Rec. 220, 337–356.
Hutton, W.C., Adams, M.A., 1982. Can the lumbar spine be crushed in heavy lifting? Spine (Phila. Pa. 1976) 7, 586–590.
Iatridis, J.C., Kumar, S., Foster, R.J., Weidenbaum, M., Mow, V.C., 1999. Shear mechanical properties of human lumbar annulus fibrosus. J. Orthop. Res. 17, 732–737.
Iatridis, J.C., Setton, L.A., Foster, R.J., Rawlins, B.A., Weidenbaum, M., Mow, V.C., 1998. Degeneration affects the anisotropic and nonlinear behaviors of human anulus fibrosus in compression. J. Biomech. 31, 535–544.
Iatridis, J.C., Setton, L.A., Weidenbaum, M., Mow, V.C., 1997a. Alterations in the mechanical behavior of the human lumbar nucleus pulposus with degeneration and aging. J. Orthop. Res. 15, 318–322.
Iatridis, J.C., Setton, L.A., Weidenbaum, M., Mow, V.C., 1997b. The viscoelastic behavior of the non-degenerate lumbar nucleus in shear. J. Biomech. 30, 1005–1013.
Iatridis, J.C., Weidenbaum, M., Setton, L.A., Mow, V.C., 1996. Is the nucleus pulposus a solid or a fluid? Mechanical behaviors of the nucleus pulposus of the human intervertebral disc. Spine (Phila. Pa. 1976) 21, 1174–1184.
Ingelmark, B.E., Ekholm, R., 1952. The compressibility of intervertebral disks; an experimental investigation on the intervertebral disk between the third and fourth lumbar vertebrae in man. Acta Soc. Med. Ups 57, 202–217.
Inoue, H., 1981. Three-dimensional architecture of lumbar intervertebral discs. Spine (Phila. Pa. 1976) 6, 139–146.
Inoue, H., Takeda, T., 1975. Three-dimensional observation of collagen framework of lumbar intervertebral discs. Acta Orthop. Scand. 46, 949–956.
Izambert, O., Mitton, D., Thourot, M., Lavaste, F., 2003. Dynamic stiffness and damping of human intervertebral disc using axial oscillatory displacement under a free mass system. Eur. Spine J. 12, 562–566.
Jamison, D., Cannella, M., Pierce, E.C., Marcolongo, M.S., 2013. A comparison of the human lumbar intervertebral disc mechanical response to normal and impact loading conditions. J. Biomech. Eng. 135, 91009.
Janevic, J., Ashton-Miller, J.A., Schultz, A.B., 1991. Large compressive preloads decrease lumbar motion segment flexibility. J. Orthop. Res. Publ. Orthop. Res. Soc. 9, 228–236.
Johannessen, W., Auerbach, J.D., Wheaton, A.J., Kurji, A., Borthakur, A., Reddy, R., Elliott, D.M., 2006. Assessment of human disc degeneration and proteoglycan content using T1 rho-weighted magnetic resonance imaging. Spine (Phila. Pa. 1976) 31, 1253–1257.
Johannessen, W., Elliott, D.M., 2005. Effects of degeneration on the biphasic material properties of human nucleus pulposus in confined compression. Spine (Phila. Pa. 1976) 30, E724–E729.
Kasra, M., Shirazi-Adl, A., Drouin, G., 1992. Dynamics of human lumbar intervertebral joints: experimental and finite-element investigations. Spine (Phila. Pa. 1976) 17, 93–102.
Kazarian, L., 1975. Creep characteristics of the human spinal column. Orthop. Clin. N. Am. 6, 3–18.
Keller, T.S., Spengler, D.M., Hansson, T.H., 1987. Mechanical behavior of the human lumbar spine. I. Creep analysis during static compressive loading. J. Orthop. Res. 5, 467–478.
Kemper, A.R., McNally, C., Duma, S.M., 2007. The influence of strain rate on the compressive stiffness properties of human lumbar intervertebral discs. Biomed. Sci. Instrum. 43, 176–181.
Keyes, D.C., Compere, E.L., 1932. The normal and pathological physiology of the nucleus pulposus of the intervertebral disc. J Bone Jt. Surg. Am. 14, 897–938.
Klisch, S.M., Lotz, J.C., 2000. A special theory of biphasic mixtures and experimental results for human annulus fibrosus tested in confined compression. J. Biomech. Eng. 122, 180–188.
Koeller, W., Funke, F., Hartmann, F., 1984a. Biomechanical behavior of human intervertebral discs subjected to long lasting axial loading. Biorheology 21, 675–686.
Koeller, W., Meier, W., Hartmann, F., 1984b. Biomechanical properties of human intervertebral discs subjected to axial dynamic compression: a comparison of lumbar and thoracic discs. Spine (Phila. Pa. 1976) 9, 725–733.
Koeller, W., Muehlhaus, S., Meier, W., Hartmann, F., 1986. Biomechanical properties of human intervertebral discs subjected to axial dynamic compression - influence of age and degeneration. J. Biomech. 19, 807–816.
Kraemer, J., Kolditz, D., Gowin, R., 1985. Water and electrolyte content of human intervertebral discs under variable load. Spine (Phila. Pa. 1976) 10, 69–71.
Lama, P., Zehra, U., Balkovec, C., 2014. Significance of cartilage endplate within herniated disc tissue. Eur. Spine J. 23, 1869–1877.
Lee, C., Goel, V., 2004. Artificial disc prosthesis: design concepts and criteria. Spine J. 4, 209S–218S.
Lemaire, J.P., Skalli, W., Lavaste, F., Templier, A., Mendes, F., Diop, A., Sauty, V., Laloux, E., 1997. Intervertebral disc prosthesis: results and prospects for the year 2000. Clin. Orthop. Relat. Res. 337, 64–76.
Lin, H.S., Liu, Y.K., Adams, K.H., 1978. Mechanical response of the lumbar intervertebral joint under physiological (complex) loading. J. Bone Jt. Surg. Am. 60, 41–55.
Liu, J., Hao, L., Suyou, L., Shan, Z., Maiwulanjiang, M., Li, S., Wang, C., Fan, S., Zhao, F., 2016. Biomechanical properties of lumbar endplates and their correlation with MRI findings of lumbar degeneration. J. Biomech. 49, 586–593.
Lorenz, M., Patwardhan, A., Vanderby, R., 1983. Load-bearing characteristics of lumbar facets in normal and surgically altered spinal segments. Spine (Phila. Pa. 1976) 8, 122–130.
Marchand, F., Ahmed, A.M., 1990. Investigation of the laminate structure of lumbar disc anulus fibrosus. Spine (Phila. Pa. 1976) 15, 402–410.
Marchand, F., Ahmed, A.M., 1989. Mechanical properties and failure mechanisms of the lumbar disc annulus. Trans. Orthop. Res. Soc. 14, 355.
Marini, G., Huber, G., Püschel, K., Ferguson, S.J., 2015. Nonlinear dynamics of the human lumbar intervertebral disc. J. Biomech. 48, 1–10.
Markolf, K., 1972. Deformation of the thoracolumbar intervertebral joints in response to external loads. J. Bone Jt. Surg. Am. 54, 511–533.
Markolf, K.K.L., Morris, J.J.M., 1974. The structural components of the intervertebral disc. J. Bone Jt. Surg. 56, 675–687.
Masouros, S.D., Parker, K.H., Hill, A.M., Amis, A.A., Bull, A.M.J., 2009. Testing and modelling of soft connective tissues of joints: a review. J. Strain Anal. Eng. Des. 44, 305–318.
McDevitt, C., 1988. Proteoglycans of the intervertebral disc. In: Ghosh, P. (Ed.), The Biology of the Intervertebral Disc. CDC Press, Boca Raton, Florida, USA, 151–171.
McMillan, D., Garbutt, G., Adams, M., 1996. Effect of sustained loading on the water content of intervertebral discs: implications for disc metabolism. Ann. Rheum. Dis. 55, 880–887.
McNally, D., Adams, M., 1992. Internal intervertebral disc mechanics as revealed by stress profilometry. Spine (Phila. Pa. 1976) 17, 66–73.
Melrose, J., Ghosh, P., 1988. The noncollagenous proteins of the intervertebral disc. In: Ghosh, P. (Ed.), The Biology of the Intervertebral Disc. CRC Press, Boca Raton, Florida, USA, 189–237.
Melrose, J., Smith, S.M., Appleyard, R.C., Little, C.B., 2008. Aggrecan, versican and type VI collagen are components of annular translamellar crossbridges in the intervertebral disc. Eur. Spine J. 17, 314–324.
Mikawa, Y., Hamagami, H., Shikata, J., Yamamuro, T., 1986. Elastin in the human intervertebral disk. A histological and biochemical study comparing it with elastin in the human yellow ligament. Arch. Orthop. Trauma Surg. 105, 343–349.
Moroney, S.P., Schultz, A.B., Miller, J.A., Andersson, G.B., 1988. Load-displacement properties of lower cervical spine motion segments. J. Biomech. 21, 769–779.
Nachemson, A., 1965. The effect of forward leaning on lumbar intradiscal pressure. Acta Orthop. Scand. 35, 314–328.
Nachemson, A., 1963. The influence of spinal movements on the lumbar intradiscal

pressure and on the tensile stresses in the annulus fibrosus. Acta Orthop. Scand. 33, 183–207.
Nachemson, A., 1960. Lumbar intradiscal pressure: experimental studies on post-mortem material. Acta Orthop. 31, 1–104.
Nachemson, A., Lewin, T., Maroudas, A., Freeman, M.A.R., 1970. In vitro diffusion of dye through the end-plates and the annulus fibrosus of human lumbar inter-vertebral discs. Acta Orthop. Scand. 41, 589–607.
Nachemson, A., Morris, J., 1964. In vivo measurements of intradiscal pressure. J. Bone Jt. Surg. 46, 1077–1092.
Nachemson, A., Morris, J., 1963. Lumbar discometry lumbar intradiscal pressure measurements in vivo. Lancet 281, 1140–1142.
Nachemson, A., Schultz, A.B., Berkson, M.H., 1979. Mechanical properties of human lumbar spine motion segments: influences of age, sex, disc level, and degeneration. Spine (Phila. Pa. 1976) 4, 1–8.
Nachemson, A.L., Evans, J.H., 1968. Some mechanical properties of the third human lumbar interlaminar ligament (ligamentum flavum). J. Biomech. 1, 211–220.
O'Connell, G., Jacobs, N., Sen, S., Vresilovic, E., 2011a. Axial creep loading and unloaded recovery of the human intervertebral disc and the effect of degeneration. J. Mech. Behav. Biomed. Mater. 4, 933–942.
O'Connell, G.D., Johannessen, W., Vresilovic, E.J., Elliott, D.M., 2007. Human internal disc strains in axial compression measured noninvasively using magnetic resonance imaging. Spine (Phila. Pa. 1976) 32, 2860–2868.
O'Connell, G.D.G., Guerin, H.L.H., Elliott, D.M., 2009. Theoretical and uniaxial experimental evaluation of human annulus fibrosus degeneration. J. Biomech. Eng. 131, 111007-1–111007-7.
O'Connell, G., Vresilovic, E., Elliott, D., 2011b. Human intervertebral disc internal strain in compression: the effect of disc region, loading position, and degeneration. J. Orthop. Res. 29, 547–555.
O'Connell, G., Malhotra, N., Vresilovic, E., Elliott, D., 2011c. The effect of discectomy and the dependence on degeneration of human intervertebral disc strain in axial compression. Spine (Phila. Pa. 1976) 36, 1765–1771.
Panagiotacopulos, N.D., Pope, M.H., Bloch, R., Krag, M.H., 1987. Water content in human intervertebral discs. Part II. Viscoelastic behaviour. Spine (Phila. Pa. 1976) 12, 918–924.
Panjabi, M., Oxland, T., Takata, K., Goel, V., Duranceau, M., Krag, M., 1993. Articular facets of the human spine quantitative three-dimensional anatomy. Spine (Phila. Pa. 1976) 10, 1298–1310.
Panjabi, M., Summers, D., Pelker, R., Videman, T., Friedlaender, G., Southwick, W., 1986. Three dimensional load displacement curves due to forces on the cervical spine. J. Orthop. Res. 4, 152–161.
Panjabi, M.M., Brand, R.A., White, A.A., 1976. Three-dimensional flexibility and stiffness properties of the human thoracic spine. J. Biomech. 9, 185–192.
Panjabi, M.M., Duranceau, J., Goel, V., Oxland, T., Takata, K., 1991. Cervical human vertebrae quantitative three-dimensional anatomy of the middle and lower regions. Spine (Phila. Pa. 1976) 16, 861–869.
Panjabi, M.M., Goel, V., Oxland, T., Takata, K., Duranceau, J., Krag, M., Price, M., 1992. Human lumbar vertebrae: quantitative three-dimensional anatomy. Spine (Phila. Pa. 1976) 17, 299–306.
Panjabi, M.M., Krag, M., Summers, D., Videman, T., 1985. Biomechanical time-tolerance of fresh cadaveric human spine specimens. J. Orthop. Res. 3, 292–300.
Panzer, M., Fice, J., Cronin, D., 2011. Cervical spine response in frontal crash. Med. Eng. Phys. 33, 1147–1159.
Patwardhan, A., Harvey, R., Carandang, G., Simonds, J., Voronov, L., Ghanayem, A., Meade, K., Gavin, T., Paxinos, O., 2003. Effect of compressive follower preload on the flexion–extension response of the human lumbar spine. J. Orthop. Res. 21, 540–546.
Patwardhan, A., Havey, R., Ghanayem, A., 2000. Load-carrying capacity of the human cervical spine in compression is increased under a follower load. Spine (Phila. Pa. 1976) 25, 1548–1554.
Patwardhan, A.G., Havey, R.M., Meade, K.P., Lee, B., Dunlap, B., 1999. A follower load increases the load carrying capacity of the lumbar spine in compression. Spine (Phila. Pa. 1976) 24, 1003–1009.
Pearcy, M.J., Hindle, R.J., 1991. Axial rotation of lumbar intervertebral joints in forward flexion. Proc. Inst. Mech. Eng. H 205, 205–209.
Perey, O., 1957. Fracture of the vertebral end-plate in the lumbar spine: an experimental biochemical investigation. Acta Orthop. Scand. 18, 1–101.
Pezowicz, C.A., Robertson, P.A., Broom, N.D., 2006. The structural basis of interlamellar cohesion in the intervertebral disc wall. J. Anat. 208, 317–330.
Pfirrmann, C., Metzdorf, A., Zanetti, M., Hodler, J., Boos, N., 2001. Magnetic resonance classification of lumbar intervertebral disc degeneration. Spine (Phila. Pa. 1976) 26, 1873–1878.
Pflaster, D.S., Krag, M.H., Johnson, C.C., Haugh, L.D., Pope, M.H., 1997. Effect of test environment on intervertebral disc hydration. Spine (Phila. Pa. 1976) 22, 133–139.
Plaue, R., Gerner, H.J., Salditt, R., 1974. Das elastomechanische Verhalten menschlicher Bandscheiben unter statischem Druck. Arch. Orthop. Unf.-Chir. 79, 139–148.
Pollintine, P., Przybyla, A.S., Dolan, P., Adams, M.A., 2004. Neural arch load-bearing in old and degenerated spines. J. Biomech. 37, 197–204.
Pooni, J., Hukins, D., Harris, P., Hilton, R., Davies, K., 1986. Comparison of the structure of human intervertebral discs in the cervical, thoracic and lumbar regions of the spine. Surg. Radiol. Anat. 8, 175–182.
Przybyla, A., Skrzypiec, D., Pollintine, P., Dolan, P., Adams, M.A., 2007. Strength of the cervical spine in compression and bending. Spine (Phila. Pa. 1976) 32, 1612–1620.
Race, A., Broom, N.D., Robertson, P., 2000. Effect of loading rate and hydration on the mechanical properties of the disc. Spine (Phila. Pa. 1976) 25, 662–669.
Roberts, S., McCall, I.W., Menage, J., Haddaway, M.J., Eisenstein, S.M., 1997. Does the thickness of the vertebral subchondral bone reflect the composition of the intervertebral disc? Eur. Spine J. 6, 385–389.
Roberts, S., Menage, J., Urban, J., 1989. Biochemical and structural properties of the cartilage end-plate and its relation to the intervertebral disc. Spine (Phila. Pa. 1976) 14, 166–174.
Roberts, S., Urban, J.P., Evans, H., Eisenstein, S.M., 1996. Transport properties of the human cartilage endplate in relation to its composition and calcification. Spine (Phila. Pa. 1976) 21, 415–420.
Rodrigues, S.A., Wade, K.R., Thambyah, A., Broom, N.D., 2012. Micromechanics of annulus-end plate integration in the intervertebral disc. Spine J. 12, 143–150.
Rolander, S.D., 1966. Motion of the lumbar spine with special reference to the stabilizing effect of posterior fusion. An experimental study on autopsy specimens. Acta Orthop. Scand. 37, 1–144.
Sato, K., Kikuchi, S., Yonezawa, T., 1999. In vivo intradiscal pressure measurement in healthy individuals and in patients with ongoing back problems. Spine (Phila. Pa. 1976) 24, 2468–2474.
Schmidt, H., Galbusera, F., Rohlmann, A., Shirazi-Adl, A., 2013. What have we learned from finite element model studies of lumbar intervertebral discs in the past four decades? J. Biomech. 46, 2342–2355.
Schneiderman, G., Flannigan, B., Kingston, S., Thomas, J., Dillin, W., WAtkins, R., 1987. Magnetic resonance imaging in the diagnosis of disc degeneration correlation with discography. Spine (Phila. Pa. 1976) 12, 276–281.
Schollmeier, G., Lahr-Eigen, R., Lewandrowski, K.U., 2000. Observations on fiber-forming collagens in the anulus fibrosus. Spine (Phila. Pa. 1976) 25, 2736–2741.
Schollum, M.L., Robertson, P.A., Broom, N.D., 2008. ISSLS prize winner: microstructure and mechanical disruption of the lumbar disc annulus. Spine (Phila. Pa. 1976) 33, 2702–2710.
Schultz, A.B., Warwick, D.N., Berkson, M.H., Nachemson, A.L., 1979. Mechanical properties of human lumbar spine motion segments - Part I: responses in flexion, extension, lateral bending, and torsion. J. Biomech. Eng. 101, 46–52.
Scoles, P.V., Linton, A.E., Latimer, B., Levy, M.E., Digiovanni, B.F., 1988. Vertebral body and posterior element morphology: the normal spine in middle life. Spine (Phila. Pa. 1976) 13, 1082–1086.
Sen, S., Jacobs, N.T., Boxberger, J.I., Elliott, D.M., 2012. Human annulus fibrosus dynamic tensile modulus increases with degeneration. Mech. Mater. 44, 93–98.
Shan, Z., Li, S., Liu, J., Mamuti, M., Wang, C., Zhao, F., 2015. Correlation between biomechanical properties of the annulus fibrosus and magnetic resonance imaging (MRI) findings. Eur. Spine J. 24, 1909–1916.
Shirazi-Adl, A., Ahmed, A.M., Shrivastava, S.C., 1986. Mechanical response of a lumbar motion segment in axial torque alone and combined with compression. Spine (Phila. Pa. 1976) 11, 914–927.
Shirazi-Adl, A., Drouin, G., 1987. Load-bearing role of facets in a lumbar segment under sagittal plane loadings. J. Biomech. 20, 601–613.
Skaggs, D.L., Weidenbaum, M., Iatridis, J.C., Ratcliffe, A., Mow, V.C., 1994. Regional variation in tensile properties and biochemical composition of the human lumbar anulus fibrosus. Spine (Phila. Pa. 1976) 19, 1310–1319.
Skrzypiec, D., Pollintine, P., Przybyla, A., Dolan, P., Adams, M., 2007a. The internal mechanical properties of cervical intervertebral discs as revealed by stress profilometry. Eur. Spine J. 16, 1701–1709.
Skrzypiec, D., Tarala, M., Pollintine, P., Dolan, P., Adams, M.A., 2007b. When are intervertebral discs stronger than their adjacent vertebrae? Spine (Phila. Pa. 1976) 32, 2455–2461.
Smeathers, J.E., Joanes, D.N., 1988. Dynamic compressive properties of human lumbar intervertebral joints: a comparison between fresh and thawed specimens. J. Biomech. 21, 425–433.
Spenciner, D., Greene, D., Paiva, J., Palumbo, M., Crisco, J.J., 2006. The multidirectional bending properties of the human lumbar intervertebral disc. Spine J 6, 248–257.
Smith, L.J., Byers, S., Costi, J.J., Fazzalari, N.L., 2008. Elastic Fibers Enhance the Mechanical Integrity of the Human Lumbar Anulus Fibrosus in the Radial Direction. Ann. Biomed. Eng. 36, 214–223.
Stanley, S.K., Ghanayem, A.J., Voronov, L.I., Havey, R.M., Paxinos, O., Carandang, G., Zindrick, M.R., Patwardhan, A.G., 2004. Flexion-extension response of the thoracolumbar spine under compressive follower preload. Spine (Phila. Pa. 1976) 29, E510–E514.
Sunni, N., Askin, G.N., Labrom, R.D., Izatt, M.T., Pearcy, M.J., Adam, C.J., 2014. The effect of repeated loading and freeze-thaw cycling on immature bovine thoracic motion segment stiffness. Proc. Inst. Mech. Eng. Part H J. Eng. Med. 228, 1100–1107.
Tan, J.S., Uppuganti, S., 2012. Cumulative multiple freeze-thaw cycles and testing does not affect subsequent within-day variation in intervertebral flexibility of human cadaveric lumbosacral spine. Spine (Phila. Pa. 1976) 37, E1238–E1242.
Tencer, A.F., Ahmed, A.M., Burke, D.L., 1982. Some static mechanical properties of the lumbar intervertebral joint, intact and injured. J. Biomech. Eng. 104, 193–201.
Tencer, A.F., Hampton, D., Eddy, S., 1995. Biomechanical properties of threaded inserts for lumbar interbody spinal fusion. Spine (Phila. Pa. 1976) 20, 2408–2414.
Thompson, J.P., Pearce, R.H., Schechter, M.T., Adams, M.E., Tsang, I.K., Bishop, P.B., 1990. Preliminary evaluation of a scheme for grading the gross morphology of the human intervertebral disc. Spine (Phila. Pa. 1976) 15, 411–415.
Veres, S.P., Robertson, P.A., Broom, N.D., 2010. The influence of torsion on disc herniation when combined with flexion. Eur. Spine J. 19, 1468–1478.
Vernon-Roberts, B., Fazzalari, N.L., Manthey, B.A., 1997. Pathogenesis of tears of the anulus investigated by multiple-level transaxial analysis of the T12-L1 disc. Spine (Phila. Pa. 1976) 22, 2641–2646.
Vernon-Roberts, B., Pirie, C.J., 1977. Degenerative changes in the intervertebral discs of the lumbar spine and their sequelae. Rheumatol. Rehabil. 16, 13–21.
Virgin, W., 1951. Experimental investigations into the physical properties of the intervertebral disc. J. Bone Jt. Surg., Br. 33B, 607–610.

Wade, K.R., Robertson, P.A., Broom, N.D., 2012a. On the extent and nature of nucleus-annulus integration. Spine (Phila. Pa. 1976) 37, 1826–1833.

Wade, K.R., Robertson, P.A., Broom, N.D., 2012b. On how nucleus-endplate integration is achieved at the fibrillar level in the ovine lumbar disc. J. Anat. 221, 39–46.

Wade, K.R., Robertson, P.A., Thambyah, A., Broom, N.D., 2015. "Surprise" loading in flexion increases the risk of disc herniation due to annulus-endplate junction failure: a mechanical and microstructural investigation. Spine (Phila. Pa. 1976) 40, 891–901.

Wade, K.R., Robertson, P.A., Thambyah, A., Broom, N.D., 2014. How healthy discs herniate. Spine (Phila. Pa. 1976) 39, 1018–1028.

Wagner, D.R., Lotz, J.C., 2004. Theoretical model and experimental results for the nonlinear elastic behavior of human annulus fibrosus. J. Orthop. Res. 22, 901–909.

White, A.A., III, 1969. Analysis of the mechanics of the thoracic spine in man: an experimental study of autopsy specimens. Acta Orthop. 40, 1–105.

Wilke, H.J., Neef, P., Caimi, M., Hoogland, T., Claes, L.E., 1999. New in vivo measurements of pressures in the intervertebral disc in daily life. Spine (Phila. Pa. 1976) 24, 755–762.

Wilke, H.J., Ressel, L., Heuer, F., Graf, N., Rath, S., 2013. Can prevention of a reherniation be investigated? Establishment of a herniation model and experiments with an anular closure device. Spine (Phila. Pa. 1976) 38, E587–E593.

Wilke, H.J., Wenger, K., Claes, L., 1998. Testing criteria for spinal implants: recommendations for the standardization of in vitro stability testing of spinal implants. Eur. Spine J. 7, 148–154.

Wu, H.C., Yao, R.F., 1976. Mechanical behavior of the human annulus fibrosus. J. Biomech. 9, 1–7.

Yamada, H., 1970. Strength of Biological Materials. Williams & Wilkins, Baltimore, MD, USA.

Yang, K.H., King, A.I., 1984. Mechanism of facet load transmission as a hypothesis for low-back pain. Spine (Phila. Pa. 1976) 9, 557–565.

Yang, K.H., Kish, V.L., 1988. Compressibility measurement of human intervertebral nucleus pulposus. J. Biomech. 21, 865.

Yingling, V.R., Callaghan, J.P., McGill, S.M., 1997. Dynamic loading affects the mechanical properties and failure site of porcine spines. Clin. Biomech. 12, 301–305.

Yoganandan, N., Ray, G., Pintar, F.A., Myklebust, J.B., Sances, A., 1989. Stiffness and strain energy criteria to evaluate the threshold of injury to an intervertebral joint. J. Biomech. 22, 135–142.

Yu, J., Fairbank, J.C.T., Roberts, S., Urban, J.P.G., 2005. The elastic fiber network of the anulus fibrosus of the normal and scoliotic human intervertebral disc. Spine (Phila. Pa. 1976) 30, 1815–1820.

Yu, J., Tirlapur, U., Fairbank, J., Handford, P., Roberts, S., Winlove, P.P., Cui, Z., Urban, J., 2007. Microfibrils, elastin fibres and collagen fibres in the human intervertebral disc and bovine tail disc. J. Anat. 210, 460–471.

Zhao, F., Pollintine, P., Hole, B.D., Dolan, P., Adams, M.A., 2005. Discogenic origins of spinal instability. Spine (Phila. Pa. 1976) 30, 2621–2630.

Zhao, F.D., Pollintine, P., Hole, B.D., Adams, M.A., Dolan, P., 2009. Vertebral fractures usually affect the cranial endplate because it is thinner and supported by less-dense trabecular bone. Bone 44, 372–379.